

# The anesthetic bupivacaine induces cardiotoxicity by targeting L-type voltage-dependent calcium channels

YaNan Gao<sup>1</sup>, Bo Chen<sup>2</sup>, Xue Zhang<sup>2</sup>,  
Rui Yang<sup>3</sup>, QingLi Hua<sup>1</sup> and BaiDong Li<sup>3</sup> 

## Abstract

**Objective:** Bupivacaine is an amide local anesthetic with possible side effects that include an irregular heart rate. However, the mechanism of bupivacaine-induced cardiotoxicity has not been fully elucidated, thus we aimed to examine this mechanism.

**Methods:** We performed electrocardiogram recordings to detect action potential waveforms in Sprague Dawley rats after application of bupivacaine, while calcium ( $\text{Ca}^{2+}$ ) currents in neonatal rat ventricular cells were examined by patch clamp recording. Western blot and quantitative real-time polymerase chain reaction assays were used to detect the expression levels of targets of interest.

**Results:** In the present study, after application of bupivacaine, abnormal action potential waveforms were detected in Sprague Dawley rats by electrocardiogram recordings, while decreased  $\text{Ca}^{2+}$  currents were confirmed in neonatal rat ventricular cells by patch clamp recording. These alterations may be attributed to a deficiency of  $\text{Ca}_v1.3$  (L-type)  $\text{Ca}^{2+}$  channels, which may be regulated by the multifunctional protein calreticulin.

**Conclusions:** The present study identifies a possible role of the calreticulin– $\text{Ca}_v1.3$  axis in bupivacaine-induced abnormal action potentials and  $\text{Ca}^{2+}$  currents, which may lead to a better understanding anesthetic drug-induced cardiotoxicity.

## Keywords

Bupivacaine, cardiotoxicity,  $\text{Ca}_v1.3$ , calreticulin, L-type  $\text{Ca}^{2+}$  channel, ventricular cells

Date received: 20 March 2020; accepted: 23 June 2020

<sup>3</sup>Cardiothoracic Surgery Department, Daqing Longnan Hospital, Daqing, People's Republic of China

## Corresponding author:

BaiDong Li, Cardiothoracic Surgery Department, Daqing Longnan Hospital, No. 35 Aiguoguo Road, Hulu District, Daqing City 163001, People's Republic of China.  
Email: libd2008v@126.com

<sup>1</sup>Anesthesiology Department, Daqing Longnan Hospital, Daqing, People's Republic of China

<sup>2</sup>ICU, Daqing Longnan Hospital, Daqing, People's Republic of China



## Introduction

Bupivacaine is an anesthetic drug with possible side effects that include low blood pressure and an irregular heart rate (HR).<sup>1,2</sup> The underlying mechanism of bupivacaine-induced cardiotoxicity has not yet been clearly reported. Given the key roles that ion channels play in regulating cardiac electrophysiological activities,<sup>3,4</sup> it is thus necessary to focus on the roles of ion channels in bupivacaine-induced arrhythmias.

L-type calcium ( $\text{Ca}^{2+}$ ) channels are widely expressed in cardiac cells, are responsible for inward  $\text{Ca}^{2+}$  current, and trigger  $\text{Ca}^{2+}$  release from the sarcoplasmic reticulum to promote excitation-contraction coupling.<sup>5,6</sup>  $\text{Ca}_v1.3$  channels belong to the  $\text{Ca}_v1$   $\text{Ca}^{2+}$  channel family, which produces L-type  $\text{Ca}^{2+}$  currents and is essential for intracellular  $\text{Ca}^{2+}$  homeostasis.<sup>7,8</sup> It is widely accepted that an abnormal  $\text{Ca}^{2+}$  level in cardiomyocytes is an important cause of arrhythmia.<sup>9,10</sup> Therefore, alterations in the action potential waveform caused by changes in  $\text{Ca}^{2+}$  currents are useful for understanding drug-induced arrhythmia.

Calreticulin is a multifunctional protein in the endoplasmic reticulum. It is widely recognized as a resident endoplasmic reticulum protein that participates in  $\text{Ca}^{2+}$  binding and storage. Recent evidence has also shown that calreticulin can be translocated to the cell surface in response to oxidative stress or other pathological or physiological stimuli, where it can regulate diverse biological processes including  $\text{Ca}^{2+}$  channel currents.<sup>11–13</sup>

In the present study, we aim to investigate the underlying mechanism of abnormal action potential waveforms induced by bupivacaine in Sprague Dawley (SD) rats. We provide evidence that bupivacaine inhibits  $\text{Ca}_v1.3$  (L-type)  $\text{Ca}^{2+}$  channels likely by promoting calreticulin expression

in rat cardiomyocytes, resulting in a decrease in  $\text{Ca}^{2+}$  current and eventually leading to arrhythmia.

## Methods

### Animal studies

We established rat models by injection of bupivacaine (1  $\mu\text{g}/\text{g}$ , 2  $\mu\text{g}/\text{g}$ , or 4  $\mu\text{g}/\text{g}$ ). All animal experiments were approved by the Experimental Animal Ethics Committee of Daqing Longnan Hospital and were conducted in compliance with animal use guidelines (SYXK (Hei) 2006-033). Eight-week-old male or female SD rats were supplied by the Medical Experimental Animal Center of Harbin Medical University (Harbin, China). Rats were housed under standard animal room conditions (temperature 20°C; humidity 55% to 60%). Food and water were freely available throughout the experiments.

### Electrocardiogram recordings

Electrocardiogram (ECG) recordings were performed on SD rats purchased from the Second Affiliated Hospital of Harbin Medical University (Harbin, China). After intraperitoneal injection of bupivacaine (1  $\mu\text{g}/\text{g}$ , 2  $\mu\text{g}/\text{g}$ , or 4  $\mu\text{g}/\text{g}$ ) or saline, SD rats (300±20 g) were intraperitoneally anesthetized with 10% chloral hydrate (3  $\mu\text{l}/\text{kg}$ ) (Merck, Kenilworth, NJ, USA), and then ECG recordings were performed using the BL-420S biosignal acquisition and processing system (Techman Soft, Sichuan Province, China). The left ventricular end diastolic pressure (LVEDP), left ventricular systolic pressure (LVSP), and HR were recorded using a pressure-digital converter. The maximal rates of pressure increase (+dp/dt) and decrease (-dp/dt) were calculated using the digitized left ventricular pressure.

### **Primary culture of rat ventricular cardiomyocytes**

Neonatal rat ventricular cells (NRVCs) were isolated from the hearts of 1- to 3-day-old newborn rats. In brief, the newborn rats were euthanized by cervical dislocation, and after all vital characteristics, such as muscle tone, disappeared, the ventricles were excised, cut into small pieces, and digested with a 0.25% trypsin solution. After the cells were isolated, NRVCs were enriched by the differential preplating method. Then, purified NRVCs were plated on 12-well plates and maintained for 48 hours in Dulbecco's Modified Eagle Medium supplemented with 10% fetal bovine serum.

### **Transfection of siRNA**

Calreticulin siRNA or siNC (100 nM) (RiboBio, Guangzhou, China) was transfected into neonatal rat cardiomyocytes for 48 hours using Lipofectamine 2000 (Invitrogen Corp., Carlsbad, CA, USA) before stimulation with bupivacaine for 24 hours.

### **Electrophysiology**

Ca<sup>2+</sup> channel currents were measured using the whole-cell patch clamp technique with an Axopatch 200 amplifier (Molecular Devices, San Jose, CA, USA) in the voltage clamp mode at room temperature. Recording pipettes with resistances between 2 and 3 M $\Omega$  were used and filled with an internal solution containing (mM) CsCl 120, MgCl<sub>2</sub> 1, HEPES 10, Mg-ATP 4, EGTA 10, and Na<sub>2</sub>-GTP 0.3, pH 7.2; the extracellular solution contained (mM): TEA-Cl 140, MgCl<sub>2</sub> 2, CaCl<sub>2</sub> 10, HEPES 10, and glucose 5, pH 7.4.

### **Western blot assay**

Whole-cell proteins were isolated from neonatal rat ventricular myocytes. Samples containing 100  $\mu$ g of protein in 10  $\mu$ L of loading buffer (Beyotime Biotechnology, Shanghai, China) were loaded and separated by electrophoresis on 8% sodium-dodecyl sulfate polyacrylamide gels. Then, proteins in the gels were transferred to polyvinylidene fluoride membranes and blocked for 1 hour using 5% nonfat milk, followed by incubation with primary antibodies to calreticulin (ab22683, Abcam, Cambridge, UK, observed band size 65 kDa) and Ca<sub>v</sub>1.3 (ab84811, Abcam, observed band size 245 kDa) overnight at 4°C on a shaker. The membranes were washed three times with 0.05% phosphate buffered saline plus 0.05% Tween and incubated with corresponding fluorescent secondary antibodies (926-32211 and 926-32210, LI-COR Biosciences, Lincoln, NE, USA) for 1 hour in the dark at room temperature. Finally, the bands on the membranes were detected with the Odyssey instrument (LI-COR Biosciences), and Odyssey software v1.2 was used to analyze and quantify the bands. The intensities of proteins were normalized to the respective  $\beta$ -actin intensity of each gel.

### **Quantitative real-time PCR**

Quantitative real-time PCR (qRT-PCR) was performed to determine the relative expression levels of genes. Total RNA was extracted from neonatal rat cardiomyocytes with the Trizol reagent (Invitrogen, USA) according to the manufacturer's instructions. The concentration and purity of total RNA were detected by a NanoDrop Spectrophotometer (NanoDrop Technologies, Wilmington, DE, USA). Afterward, a High-Capacity cDNA Reverse Transcription Kit (Applied Biosystems,

Foster City, CA, USA) was used to synthesize cDNA. qRT-PCR was performed using the SYBR Green PCR Master Mix Kit (Applied Biosystems, USA). GAPDH was used as an internal control. Finally, the results were calculated using the  $2^{-\Delta\Delta CT}$  method. The primer sequences were as follows: GAPDH: forward 5'-AACGACCCCTTCATTGAC CTC-3' and reverse 5'-CCTTGACTGTGC CGTTGAACT-3'; calreticulin: forward 5'-ATCATGTTTGGTCCCGACATC-3' and reverse 5'-TCATCCTTGCAACGGATGT C-3'; and Ca<sub>v</sub>1.3: forward 5'-AGCCAACA GTGACAACAAGG-3' and reverse 5'-TT CAACTCCGAGATCCTTCG-3'.

### *Statistical analysis*

Statistical analyses were performed using GraphPad 6 software (GraphPad Software Inc., San Diego, CA, USA). Statistical comparisons among experimental groups were evaluated using one-way analysis of variance (ANOVA) followed by a Bonferroni post-hoc test. Data are expressed as the mean±SEM. P values less than 0.05 were considered significant.

### *Ethics approval*

All animal experiments performed in this study were approved by the Experimental Animal Ethics Committee of Daqing Longnan Hospital and were conducted in compliance with the animal use guidelines (SYXK (Hei) 2006-033).

## **Results**

### *The effect of bupivacaine on rat electrocardiogram recordings*

To determine the possible effect of bupivacaine on the action potential waveform, we examined a series of bupivacaine concentrations (1 µg/g, 2 µg/g, and 4 µg/g) in SD rats.

The ECG results showed that chronic treatment with bupivacaine (1 µg/g, 2 µg/g, or 4 µg/g) significantly affected the action potential waveform of SD rats (Figure 1a). Meanwhile, three typical types of ventricular arrhythmia occurred in rats treated with bupivacaine: premature ventricular contraction, ventricular tachycardia, and ventricular fibrillation (Figure 1b). The arrhythmic duration was significantly longer in rats treated with bupivacaine than in the control animals (Figure 1c). Therefore, the cardiac function of the SD rats was examined to evaluate the effect of bupivacaine. The results in Figure 1d show that bupivacaine induced a significant decrease in HR, LVSP, and ± dt/dp but not in LVEDP, which suggests that bupivacaine has a significant influence on the action potential waveform and heart rhythm of SD rats. Additionally, the effect of bupivacaine on heart function in rats was determined by ultrasound. As depicted in Figure 1e, different concentrations of bupivacaine could inhibit the heart function of rats, including the ejection fraction and fractional shortening.

### *Bupivacaine inhibits the calcium current of neonatal rat ventricular cells*

To further explore the causes of arrhythmia induced by bupivacaine, patch-clamp recordings were used to detect the effects of different concentrations of bupivacaine on L-type Ca<sup>2+</sup> channel currents. Figure 2a shows representative L-type Ca<sup>2+</sup> channel currents, which indicate that bupivacaine significantly inhibited L-type Ca<sup>2+</sup> currents in a concentration-dependent manner. The normalized current–voltage (I-V) relationship in Figure 2b was constructed after normalizing the currents at various test potentials to the maximum current and dividing by cell membrane capacitance. The results show that bupivacaine obviously inhibited the

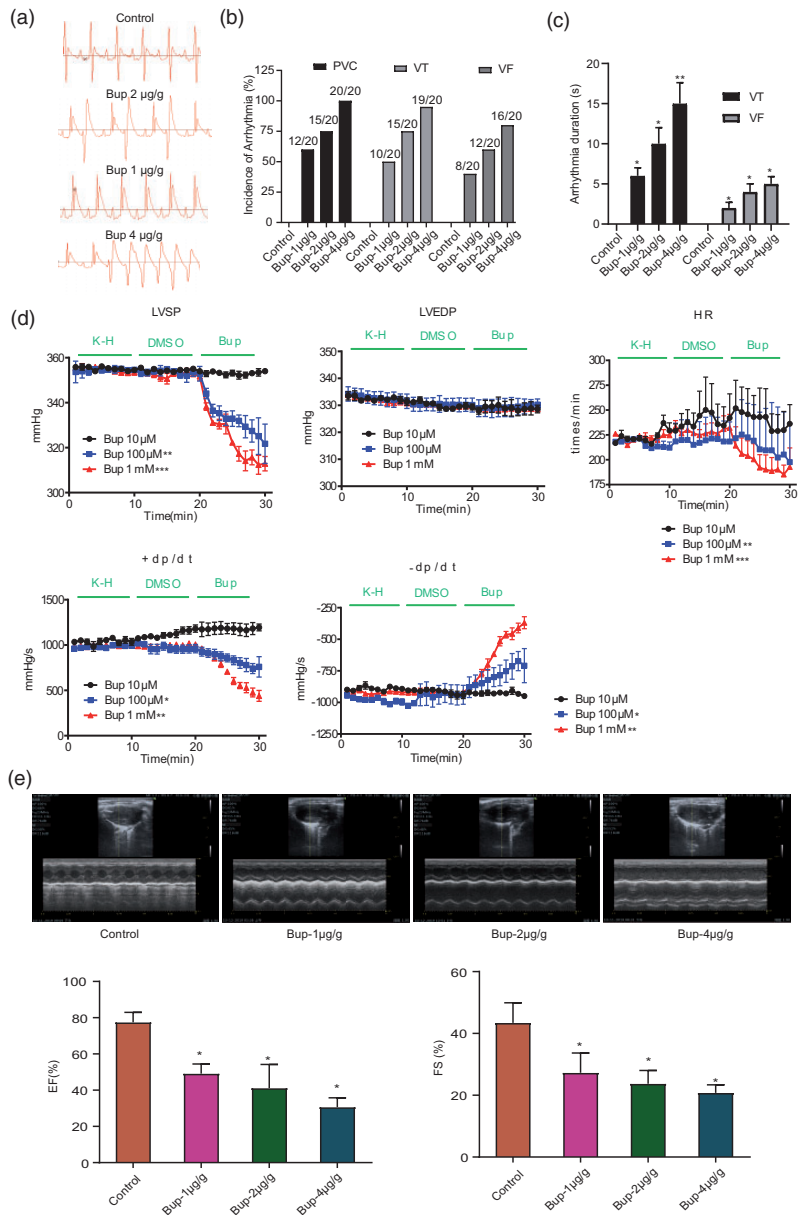


**Figure 1.** Effect of bupivacaine on rat electrocardiograms. (a) Representative action potential waveforms of Sprague Dawley rats with or without chronic treatment with bupivacaine (1  $\mu\text{g/g}$ , 2  $\mu\text{g/g}$ , or 4  $\mu\text{g/g}$ ). (b) Statistical analysis of the incidence of arrhythmias. (c) Duration (in seconds) of arrhythmias. (d) Bupivacaine induces a significant decrease in the heart rate, left ventricular systolic pressure, and maximal rate of pressure increase or decrease but does not affect left ventricular end diastolic pressure (n=20). \*\*P<0.01 or \*\*\*P<0.001 vs. control group. (e) The effect of bupivacaine on rat heart function determined by ultrasound. (n=20). \*P<0.05 vs. the control group. Bup, bupivacaine; PVC, premature ventricular contraction; VT, ventricular tachycardia; VF, ventricular fibrillation; LVSP, left ventricular systolic pressure; LVEDP, left ventricular end diastolic pressure; HR, heart rate; +/- dp/dt, maximal rates of pressure increase and decrease; EF, ejection fraction; FS, fractional shortening.

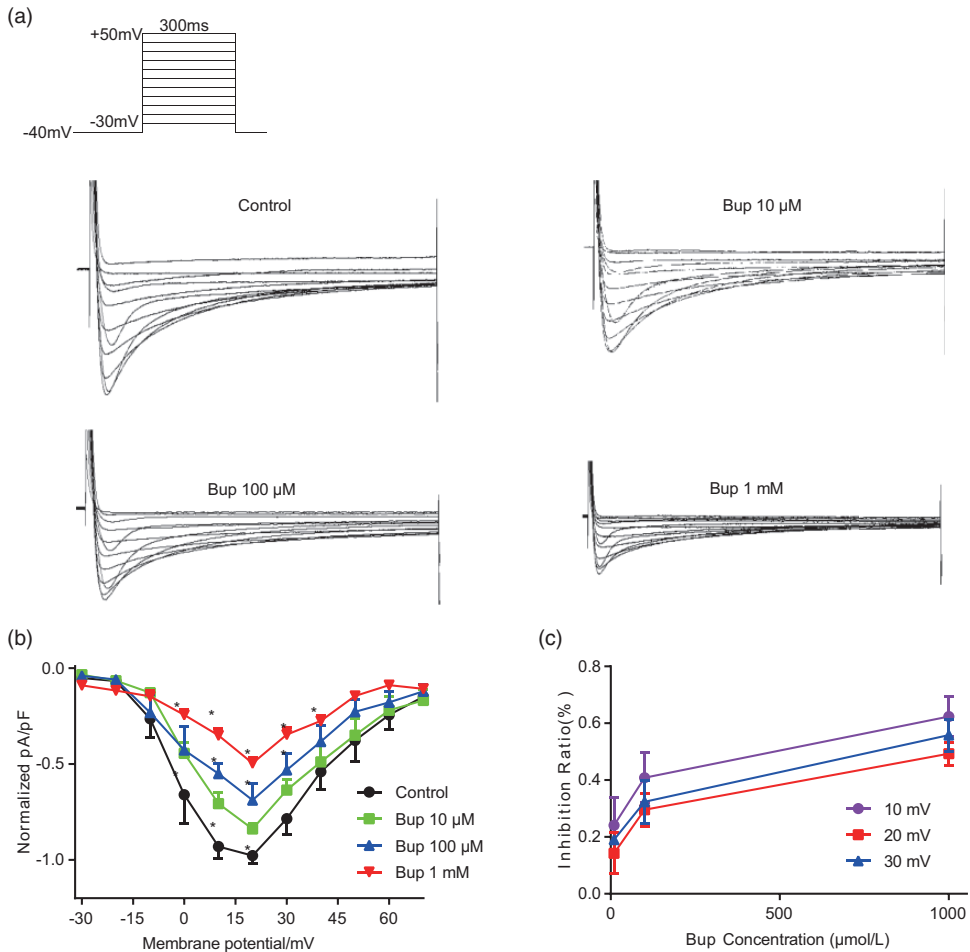


**Figure 2.** Bupivacaine inhibits calcium ( $\text{Ca}^{2+}$ ) currents in neonatal rat ventricular cells. (a) Representative  $\text{Ca}^{2+}$  currents of neonatal rat ventricular cells with or without chronic bupivacaine treatment (10  $\mu\text{M}$ , 100  $\mu\text{M}$ , or 1 mM). (b) A statistical analysis of  $\text{Ca}^{2+}$  currents shows the normalized current-voltage relationships in the absence and presence of bupivacaine. (c) The inhibition of  $\text{Ca}^{2+}$  currents by bupivacaine ( $n=11$ ). \* $P<0.05$  vs. the control group. Bup, bupivacaine.

L-type  $\text{Ca}^{2+}$  channel I-V relationship, and the inhibition ratio is shown in Figure 2c.

### The effect of bupivacaine on $\text{Ca}_v1.3$ and calreticulin

$\text{Ca}_v1.3$  channels are responsible for inward  $\text{Ca}^{2+}$  current, thus we focused on the expression level of  $\text{Ca}_v1.3$  in neonatal rat cardiomyocytes after administration of

bupivacaine (10  $\mu\text{M}$ , 100  $\mu\text{M}$ , or 1 mM). Figure 3a–b show that bupivacaine inhibited the mRNA and protein expression levels of  $\text{Ca}_v1.3$  in a concentration-dependent manner. To further explore the potential mechanism of bupivacaine-induced  $\text{Ca}_v1.3$  deficiency, we detected the expression levels of calreticulin. The results showed that the mRNA and protein expression levels of

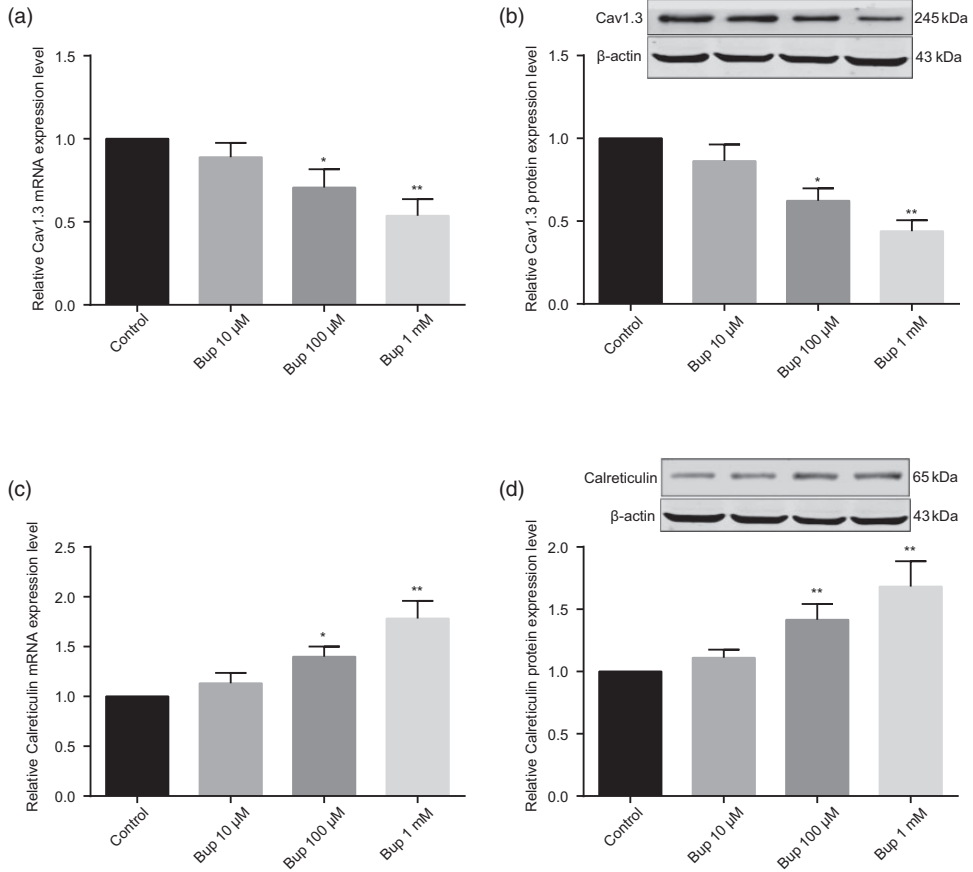


**Figure 3.** Effect of bupivacaine on  $Ca_v1.3$  and calreticulin expression. (a) Bupivacaine inhibits  $Ca_v1.3$  mRNA expression in a concentration-dependent manner. (b) Bupivacaine inhibits  $Ca_v1.3$  protein expression in a concentration-dependent manner. (c) Bupivacaine increases calreticulin mRNA expression in a concentration-dependent manner. (d) Bupivacaine increases calreticulin protein expression in a concentration-dependent manner ( $n=6$ ). \* $P < 0.05$  or \*\* $P < 0.01$  vs. the control group. Bup, bupivacaine.

calreticulin were negatively correlated with the bupivacaine concentration in  $Ca_v1.3$  channels. Therefore, bupivacaine promotes the mRNA and protein expression in a concentration-dependent manner (Figure 3c–d).

### Knockdown of calreticulin partially reversed $Ca_v1.3$ deficiency

The alteration of calreticulin expression led us to investigate the possible relationship between calreticulin and  $Ca_v1.3$  channels.

First, we knocked down calreticulin expression by siRNA. Figure 4a–b show the efficiency of siRNA knockdown. Transfection with si-calreticulin significantly reduced the mRNA (Figure 4a) and protein expression levels (Figure 4b) of calreticulin. We found that calreticulin knockdown could partially reverse the bupivacaine-induced  $Ca_v1.3$  deficiency of both mRNA and protein expression (Figure 4c–d). Moreover, calreticulin knockdown partially reversed the decreased  $Ca^{2+}$  current caused by bupivacaine, as shown in Figure 4e. Therefore, the

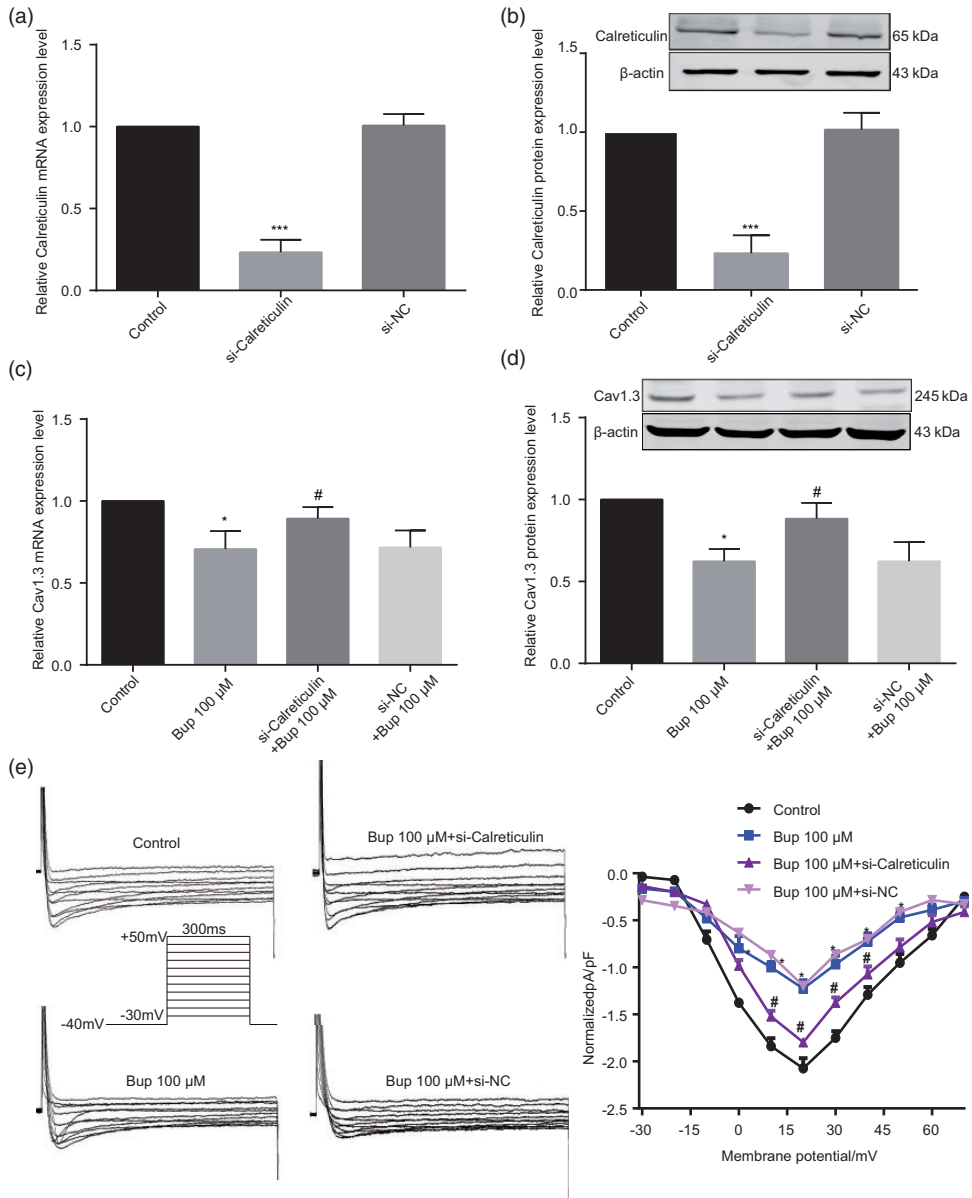


**Figure 4.** Knockdown of calreticulin partially reverses  $\text{Ca}_V1.3$  deficiency. (a) The efficiency of calreticulin siRNA knockdown was determined by qRT-PCR and (b) western blotting. (c) Calreticulin knockdown partially reversed the bupivacaine-induced decrease in  $\text{Ca}_V1.3$  mRNA. (d) and protein expression ( $n=6$ ). \* $P<0.05$  or \*\*\* $P<0.001$  vs. the control group, # $P<0.05$  vs. 100  $\mu\text{M}$  bupivacaine. (e) Calreticulin knockdown partially reversed the bupivacaine-induced decrease in  $\text{Ca}^{2+}$  current induced by bupivacaine ( $n=11$ ). \* $P<0.05$  vs. the control group, # $P<0.05$  vs. 100  $\mu\text{M}$  bupivacaine. Bup, bupivacaine.



above evidence suggests that a strong relationship exists between calreticulin and  $\text{Ca}_V1.3$  channels regarding bupivacaine-induced cardiotoxicity.

## Discussion

Heart arrhythmia may predispose individuals to complications such as stroke or heart failure and can eventually lead to sudden death.<sup>14,15</sup> The side effects of clinical drugs include cardiotoxicity, and the most common symptom of cardiotoxicity is arrhythmia.<sup>16–18</sup> Drug inhibition or blockade of ion channels is the most common treatment for heart arrhythmia.<sup>19,20</sup> Therefore, changes in action potential waveforms because of alterations in ion currents are useful for understanding drug-induced arrhythmia.

Bupivacaine, an anesthetic drug, has been reported to induce an irregular HR,<sup>1</sup> but the underlying mechanism is unknown. Given the key roles that ion channels play in regulating cardiac electrophysiological activities, it is thus necessary to focus on the roles of ion channels in bupivacaine-induced arrhythmias.

In this study, we characterized the role of the calreticulin– $\text{Ca}_V1.3$  axis in bupivacaine-induced abnormal action potentials in SD rats and  $\text{Ca}^{2+}$  currents in neonatal rat ventricular cells. We observed that the mRNA and protein expression levels of  $\text{Ca}_V1.3$  were dramatically decreased in the presence of bupivacaine in neonatal rat ventricular cells, which could be attributed to the increased expression levels of calreticulin. However, knockdown of calreticulin reversed these effects. To the best of our knowledge, the current study is the first to present new insights into the mechanism of bupivacaine-induced arrhythmias. Additionally, the results suggest that the use of bupivacaine as an anesthetic should be avoided when studying phenomena such as arrhythmia; however, if it is used as an

anesthetic, its interference with the experimental results should be excluded.

## Conclusion

This study revealed that the calreticulin– $\text{Ca}_V1.3$  axis plays a crucial role in bupivacaine-induced cardiotoxicity in cellular and animal models. Thus, drugs that block or reduce  $\text{Ca}^{2+}$  current may offer novel approaches for the prevention of cardiac arrhythmias caused by bupivacaine.

## Authors' contributions

GYN was mainly responsible for designing the research and performing real-time PCR assays and data analysis. CB and ZX mainly performed the western blotting assays and patch clamp experiments. YR and HQL were mainly responsible for the animal studies and electrocardiogram recordings. LBD was responsible for the writing and revision of the manuscript. All authors have read and approved the manuscript for submission.

## Availability of data and materials

The data and graphs used in the present study are available from the corresponding authors on reasonable request.

## Declaration of conflicting interest

The authors declare that there is no conflict of interest.

## Funding

This research received no specific grant from any funding agency in the public, commercial, or not-for-profit sectors.

## ORCID iD

BaiDong Li  <https://orcid.org/0000-0001-5628-6958>

## References

1. Partownavid P, Umar S, Li J, et al. Fatty acid oxidation and calcium homeostasis are involved in the rescue of bupivacaine-

- induced cardiotoxicity by lipid emulsion in rats. *Crit Care Med* 2012; 40: 2431–2437. DOI: 10.1097/CCM.0b013e3182544f48.
2. Liu L, Jin Z, Cai X, et al. Comparative regimens of lipid rescue from bupivacaine-induced asystole in a rat model. *Anesth Analg* 2019; 128: 256–263. DOI: 10.1213/ANE.0000000000003711.
  3. Camerino DC, Tricarico D and Desaphy JF. Ion channel pharmacology. *Neurotherapeutics* 2007; 4: 184–198. DOI: 10.1016/j.nurt.2007.01.013.
  4. Zhang YY, Li G, Che H, et al. Characterization of functional ion channels in human cardiac c-kit+ progenitor cells. *Basic Res Cardiol* 2014; 109: 407. DOI: 10.1007/s00395-014-0407-z.
  5. Yamakage M and Namiki A. Calcium channels—basic aspects of their structure, function and gene encoding; anesthetic action on the channels—a review. *Can J Anaesth* 2002; 49: 151–164. DOI: 10.1007/BF03020488.
  6. Eisner DA, Caldwell JL, Kistamas K, et al. Calcium and excitation-contraction coupling in the heart. *Circ Res* 2017; 121: 181–195. DOI: 10.1161/CIRCRESAHA.117.310230.
  7. Singh A, Gebhart M, Fritsch R, et al. Modulation of voltage- and Ca<sup>2+</sup>-dependent gating of CaV1.3 L-type calcium channels by alternative splicing of a C-terminal regulatory domain. *J Biol Chem* 2008; 283: 20733–20744. DOI: 10.1074/jbc.M802254200.
  8. Fourbon Y, Gueguinou M, Felix R, et al. Ca (2+) protein alpha 1D of CaV1.3 regulates intracellular calcium concentration and migration of colon cancer cells through a non-canonical activity. *Sci Rep* 2017; 7: 14199. DOI: 10.1038/s41598-017-14230-1.
  9. Souza DS, Menezes-Filho JER, Santos-Miranda A, et al. Calcium overload-induced arrhythmia is suppressed by farnesol in rat heart. *Eur J Pharmacol* 2019; 859: 172488. DOI: 10.1016/j.ejphar.2019.172488.
  10. Mohamed BA, Hartmann N, Tirilomis P, et al. Sarcoplasmic reticulum calcium leak contributes to arrhythmia but not to heart failure progression. *Sci Transl Med* 2018; 10: eaan0724. DOI: 10.1126/scitranslmed.aan0724.
  11. Wang WA, Groenendyk J and Michalak M. Calreticulin signaling in health and disease. *Int J Biochem Cell Biol* 2012; 44: 842–846. DOI: 10.1016/j.biocel.2012.02.009.
  12. Gold LI, Eggleton P, Sweetwyne MT, et al. Calreticulin: non-endoplasmic reticulum functions in physiology and disease. *FASEB J* 2010; 24: 665–683. DOI: 10.1096/fj.09-145482.
  13. Karnabi E, Qu Y, Yue Y, et al. Calreticulin negatively regulates the surface expression of Cav1.3 L-type calcium channel. *Biochem Biophys Res Commun* 2013; 437: 497–501. DOI: 10.1016/j.bbrc.2013.06.023.
  14. Martin CA, Matthews GD and Huang CL. Sudden cardiac death and inherited channelopathy: the basic electrophysiology of the myocyte and myocardium in ion channel disease. *Heart* 2012; 98: 536–543. DOI: 10.1136/heartjnl-2011-300953.
  15. Moccia F, Lodola F, Stadiotti I, et al. Calcium as a key player in arrhythmogenic cardiomyopathy: adhesion disorder or intracellular alteration? *Int J Mol Sci* 2019; 20: 3986. DOI: 10.3390/ijms20163986.
  16. Bauckneht M, Ferrarazzo G, Fiz F, et al. Doxorubicin effect on myocardial metabolism as a prerequisite for subsequent development of cardiac toxicity: a translational (18)F-FDG PET/CT observation. *J Nucl Med* 2017; 58: 1638–1645. DOI: 10.2967/jnumed.117.191122.
  17. Kuok KI, In Ng PC, Ji X, et al. Supramolecular strategy for reducing the cardiotoxicity of bedaquiline without compromising its antimycobacterial efficacy. *Food Chem Toxicol* 2018; 119: 425–429. DOI: 10.1016/j.fct.2017.12.022.
  18. Zhi D, Feng PF, Sun JL, et al. The enhancement of cardiac toxicity by concomitant administration of Berberine and macrolides. *Eur J Pharm Sci* 2015; 76: 149–155. DOI: 10.1016/j.ejps.2015.05.009.
  19. Tang L, Gamal El-Din TM, Lenaes MJ, et al. Structural basis for diltiazem block of

- a voltage-gated  $\text{Ca}^{2+}$  channel. *Mol Pharmacol* 2019; 96: 485–492. DOI: 10.1124/mol.119.117531.
20. Chen IS, Liu C, Tateyama M, et al. Non-sedating antihistamines block G-protein-gated inwardly rectifying  $\text{K}^{(+)}$  channels. *Br J Pharmacol* 2019; 176: 3161–3179. DOI: 10.1111/bph.14717.